2010 IEEE International Conference on Robotics and Automation
Anchorage Convention District
May 3-8, 2010, Anchorage, Alaska, USA

Integrated Controller For An Over–Constrained Cable Driven Parallel Manipulator: KNTU CDRPM

Alaleh Vafaei, Mohammad M. Aref and Hamid D. Taghirad

Abstract— **This paper presents an approach to the control of the KNTU CDRPM using an integrated control scheme. The goal in this approach is achieving accurate trajectory tracking while assuring positive tension in the cables. By the proposed controller, the inherent nonlinear behavior of the cable and the target tracking errors are simultaneously compensated. In this paper asymptotic stability analysis of the close loop system is studied in detail. Moreover, it is shown that the integrated control strategy reduces the tracking error by 80% compared to that of a single loop controller in the considered manipulator. The closed–loop performance of the control topology is analyzed by a simulation study that is performed on the manipulator. The simulation study verifies that the proposed controller is not only promising to be implemented on the KNTU CDRPM, but also being suitable for other cable driven manipulators.**

I. Introduction

Increasing performance requirements necessitates design of new types of manipulators working in a larger dexterous workspace with higher accelerations. Parallel manipulators can generally perform better than serial manipulators in terms of stringent stiffness and acceleration requirements[1] [2]. However, limited workspace and existence of many singular regions inside the workspace of a typical parallel manipulator, limit the use of parallel manipulators in various applications. In the case of *cable driven redundant parallel manipulators* (CDRPM), the conventional linear actuators of parallel manipulators are replaced with electrical powered cable drivers. This novel engineering design idea leads immediately to a wider workspace, and higher accelerations of the moving platform due to the fact of using lighter moving parts [3]. However, forward kinematics of parallel manipulators such as CDRPM's are very complicated and difficult to solve [4]. Cables are sagged under compression forces [5], and therefore, to achieve tension forces in the cables throughout the whole *dexterous workspace*, the moving platform must be designed over-constrained [6]. In this case m = n + 2 cables are proposed to be used in order to *dextrously* move the redundant actuated end–effector in an n-dimensional space [7]. Redundancy resolution is needed to assure tension force along each cable, however, this is usually computationally expensive [8]. The KNTU CDRPM uses a novel design to achieve high stiffness, accurate positioning for high-speed maneuvers.

This research is supported by K.N.Toosi University of Technology under Grant MP1853.

Authors are with the Advanced Robotics and Automated Systems (ARAS), Faculty of Electrical and Computer Engineering, K.N. Toosi University of Technology, P.O. Box 16315-1355, Tehran, Iran, E-mails: vafaei@ee.kntu.ac.ir, m_aref@sina.kntu.ac.ir and taghirad@kntu.ac.ir.

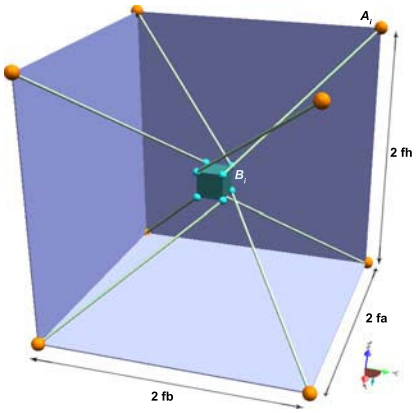

Fig. 1. The KNTU CDRPM, a perspective view

This paper presents an approach to the control of the CDRPMs using an integrated control scheme to achieve a stringent tracking performance while all the cables are in tension for such maneuvers. Control schemes for parallel manipulators are grouped in two classifications in the literature. The first one classifies the control methodologies in two frameworks. One is to design a controller based on the leg space or joint space coordinates and the other is based on the workspace or task space coordinates [9], [10]. Most of the controllers are designed based on the joint space coordinates [11], [12]. The other framework is based on the workspace coordinates [10], [2]. The second classification sets the schemes in two categories: model–based and non model–based schemes [11],non model–based controls such as *Proportional–Integral–Derivative* (PID) control [11], [13], fuzzy logic control [14] and neural network control [15]; and model–based controls such as impedance control [16] and adaptive control [17], etc. Nevertheless, there are few researches focused on the position control of Cable Driven Redundant Parallel Manipulators (CDRPM). There are two general schemes in this field; The first one works on the joint space coordinate, the length of the cables are measured and then controlled to reach the desired cable length corresponding to a desired position of an end–effector [18], [19]. Kawamura et al. proved that such a controller can guarantee the convergence of the motion of the end–effector to a desired trajectory. However, as studied in the control section, the joint space controller confronts some problems in the tracking performance [19], [5]. On the other hand, the second scheme controls the pose of the end–effector based on the dynamics described by a feedback from a 6DOF position or acceleration sensor in the task space or

workspace coordinates. For instance, a workspace controller is proposed which uses the position of the end–effector to acquire the pose of the moving platform [20] for an under-constrained suspended CDRPM.

This paper presents a different control topology examined for possible implementation on KNTU CDRPM using an integrated control scheme. The proposed controller structure guarantees fully tension forces on the cables, in a more trusted fashion, and is capable to fulfill the stringent positioning requirements for these type of manipulators. This paper is organized as follows. In section II the inverse kinematics and the Jacobian is derived first. Subsection II-C recalls dynamic modeling of the KNTU CDRPM. The integrated control with on–line gravity compensation is introduced in section III-A accompanying with the proof of stability and simulation analysis. The proposed redundancy resolution scheme is examined in section III-B, and finally, the concluding remarks and contributions of this work are enlightened in the last section.

II. Kinematics and Dynamics

A. Kinematics

The KNTU Cable Driven Redundant Parallel Manipulator is illustrated in figure 1. This figure shows a spatial six degrees of freedom manipulator with two degrees of redundancy. This robot has eight identical cable limbs. The cable driven limbs are modeled as spherical-prismatic-spherical(SPS) joints, for cables can only bear tension force and not radial or bending force. Two cartesian coordinate systems $A(x, y, z)$ and $B(u, v, w)$ are attached to the fixed base and the moving platform. Points $A_1, A_2, \ldots, A_8$ lie on the fixed cubic frame and $B_1, B_2, \ldots, B_8$ lie on the moving platform. The origin O of the fixed coordinate system is located at the centroid of the cubic frame. Similarly, the origin G of the moving coordinate system is located at centroid of the cubic moving platform. The transformation from the moving platform to the fixed base can be described by a position vector $\overrightarrow{g} = \overrightarrow{OG}$ and a 3×3 rotation matrix ${}^{A}R_{B}$. Consider that a_i and ${}^{B}b_i$ denote the position vectors of points A_i and B_i in the coordinate system A and B, respectively. Although in the analysis of the KNTU CDRPM, all the attachment points, are considered to be arbitrary, the geometric and inertial parameters given in table I are used in the simulations. Similar to other parallel manipulators, CDRPM has a complicated forward kinematic solution [4]. However, the inverse kinematic analysis is sufficient for dynamic modeling. For inverse kinematic analysis of the cable driven parallel manipulator, it is assumed that the position and orientation of the moving platform $x = [x_G, y_G, z_G]^T, {}^{A}R_{B}$ are given and the problem is to find the joint variable of the CDRPM, $\boldsymbol{L} = [L_1, L_2, \ldots, L_8]^T$. From the geometry of the manipulator as illustrated in figure 2 the following vector loops can be derived:

$$ {}^{A}\overrightarrow{A_iB_i} + {}^{A}\overrightarrow{\boldsymbol{a}_i} = {}^{A}\overrightarrow{\boldsymbol{g}} + \boldsymbol{E}_i \qquad (1) $$

in which, the vectors $\boldsymbol{g}, \boldsymbol{E}_i$, and $\boldsymbol{a}_i$ are illustrated in figure 2. The length of the i'th limb is obtained through taking the dot product of the vector $\overrightarrow{A_iB_i}$ with itself. Therefore, for $i = 1, 2, \ldots, 8$:

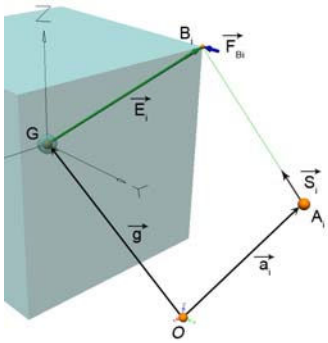

Fig. 2. ith Attachment point on the moving platform and related vectors

$$ L_i = \left\{ [\boldsymbol{g} + \boldsymbol{E}_i - \boldsymbol{a}_i]^T [\boldsymbol{g} + \boldsymbol{E}_i - \boldsymbol{a}_i] \right\}^{\frac{1}{2}} . \qquad (2) $$

B. Jacobian

Jacobian analysis plays a vital role in the study of robotic manipulators [21]. Let the actuated joint variable be denoted by a vector $\boldsymbol{L}$ and the location of the moving platform be described by a vector $\boldsymbol{x}$. Then the kinematic constrains imposed by the limbs can be written in the general form $\boldsymbol{f}(\boldsymbol{x}, \boldsymbol{L}) = 0$ by differentiating with respect to time, we obtain a relationship between the input joint rates and the end-effector output velocity as:$J_x \dot{\boldsymbol{x}} = J_L \dot{\boldsymbol{L}}$ where $J_{\boldsymbol{x}} = \frac{\partial \boldsymbol{f}}{\partial \boldsymbol{x}}$ and $J_{\boldsymbol{L}} = -\frac{\partial \boldsymbol{f}}{\partial \boldsymbol{L}}$. The derivation above leads to two separate Jacobian matrices Hence the overall Jacobian matrix J can be written as:

$$ \dot{\boldsymbol{L}} = \boldsymbol{J} \cdot \dot{\boldsymbol{x}} \qquad (3) $$

where $\boldsymbol{J} = \boldsymbol{J}_L^{-1} \boldsymbol{J}_{\boldsymbol{x}}$. Jacobian matrix not only reveals the relation between the joint velocities $\dot{\boldsymbol{L}}$ and the moving platform velocities $\dot{\boldsymbol{x}}$, but also constructs the transformation needed to find the actuator forces $\boldsymbol{\tau}$ from the forces acting on the moving platform $\boldsymbol{F}$. When J_L is singular and the null space of J_L is not empty, there exist some nonzero $\dot{\boldsymbol{L}}$ vectors that result zero $\dot{\boldsymbol{x}}$ vectors which called serial type singularity and when J_x becomes singular, there will be a non-zero twist $\dot{\boldsymbol{x}}$ for which the active joint velocities are zero. This singularity is called parallel type singularity [22].

TABLE I
Geometric and Inertial Parameters of the KNTU CDRPM

Description	Quantity
f_a: Fixed cube half length	$1\ m$
f_b: Fixed cube half width	$2\ m$
f_h: Fixed cube half height	$0.5\ m$
C : The moving platform cube half dimension	$0.1\ m$
M: The moving platform mass	$5\ Kg$
I: The moving platform moment of inertia	$0.033\ Kg \cdot m^2$
ρ: The limb density per length	$0.007\ Kg/m$

In this section we investigate the Jacobian of the CDRPM platform shown in figure 1. For this manipulator, the input vector is given by $\boldsymbol{L} = [L_1, L_2, \ldots, L_8]^T$, and the output vector can be described by the velocity of the centroid G and the angular velocity of the moving platform as follows:

$$\dot{\boldsymbol{x}} = \begin{bmatrix} \boldsymbol{V}_G \\ \boldsymbol{\omega}_G \end{bmatrix} \tag{4}$$

Jacobian matrix of a parallel manipulator is defined as the transformation matrix that converts the moving platform velocities to the joint variable velocities, as shown in equation 3. Therefore, the CDRPM Jacobian matrix J is a non-square 8×6 matrix. The Jacobian matrix can be derived by formulating a velocity loop-closure equation for each limb[23].

$$\boldsymbol{J} = \left[\begin{array}{c|c} \hat{\boldsymbol{S}}_1^T & (\boldsymbol{E}_1 \times \hat{\boldsymbol{S}}_1)^T \\ \hat{\boldsymbol{S}}_2^T & (\boldsymbol{E}_2 \times \hat{\boldsymbol{S}}_2)^T \\ \vdots & \vdots \\ \hat{\boldsymbol{S}}_8^T & (\boldsymbol{E}_8 \times \hat{\boldsymbol{S}}_8)^T \end{array}\right] \tag{5}$$

C. Dynamics

Newton-Euler method is used for dynamic modeling of CDRPM. According to acceleration of rotating velocity vector [23], the Newton-Euler equations for varying mass cable results into:

$$\boldsymbol{F}_{\text{Bi}} = \frac{-1}{2}\rho L_i^2[\dot{L}_i\boldsymbol{\omega}_i \times \hat{\boldsymbol{S}}_i + \dot{\boldsymbol{\omega}}_i \times \hat{\boldsymbol{S}}_i + \omega_i \times (\boldsymbol{\omega}_i \times \hat{\boldsymbol{S}}_i)] - \frac{\rho}{2}(\dot{L}_i^{\,2} + L_i\ddot{L}_i)\hat{\boldsymbol{S}}_i + \boldsymbol{F}_{\text{Ai}} \tag{6}$$

Where, $\boldsymbol{F}_{\text{Bi}}$, $\boldsymbol{F}_{\text{Ai}}$, $\dot{L}_i$, $\hat{\boldsymbol{S}}_i$, $\boldsymbol{\omega}_i$ and $\dot{\boldsymbol{\omega}}_i$ are resultant acting force on the each moving attachment point, acting forces on the A_i fixed joint, cable linear velocity along its straight, the unit vector on ith cable straight as shown in figure 2, the ith cable angular velocity about the fixed attachment point and the ith cable angular acceleration about the fixed attachment point, respectively. By using light weight cables such as the ones used in this manipulator, the gravity force effects on the cables can be ignored compared to the dynamic induced forces [24]. The cable tension force applied by cable driver unit, F_{Ai}^S, can be represented by:

$$\boldsymbol{F}_{\text{Ai}}^S = -\boldsymbol{\tau} \tag{7}$$

Relations between actuator forces and the end-effector affected forces had been studied in cable-affected forces. Writing the Newton-Euler equations for the moving platform describes the relation between forces, torques and acceleration of the moving platform as following:

$$M\ddot{\boldsymbol{x}} = \boldsymbol{F}_D + \boldsymbol{G} + \sum_{i=1}^{m} \boldsymbol{F}_{\text{Bi}} \tag{8}$$

$$\boldsymbol{I}_G\ddot{\boldsymbol{\theta}} = \boldsymbol{\tau}_D - \sum_{i=1}^{m} \boldsymbol{E}_i \times \boldsymbol{F}_{\text{Bi}} \tag{9}$$

In which, M and $\boldsymbol{I}_G$ are moving platform mass and moment of inertia and m is number of the cables. $\boldsymbol{G}$ is effect of gravity force on the end-effector, $\boldsymbol{F}_D$ and $\boldsymbol{\tau}_D$ are disturbance forces and torques effects on the moving platform with respect to the fixed frame coordinate. Also, $\boldsymbol{F}_{\text{Bi}}$ is calculated by the equation 6. Angular and linear acceleration of each cable $\dot{\boldsymbol{\omega}}_i$ and $\dot{L}_i$ in equation 6, depend on the end-effector acceleration, which makes the dynamic equations implicit. Therefore, equations 8 and 9 can be viewed as an implicit 6×1 vector differential equations of the form:

$$\boldsymbol{f}(\boldsymbol{x}, \dot{\boldsymbol{x}}, \ddot{\boldsymbol{x}}, \mathcal{F}_D, \boldsymbol{\tau}) = 0 \tag{10}$$

in which, $\mathcal{F}_D = [\boldsymbol{F}_D, \boldsymbol{\tau}_d]^T$ is the vector disturbance wrench. The governing motion equations of the manipulator can be implemented for dynamic simulation of the system. For dynamic simulation, it is assumed that the actuator forces $\boldsymbol{\tau}(t)$, are given and the manipulator motion trajectory $\boldsymbol{x}(t)$, is needed to be determined. It is shown that the obtained implicit equations can be converted to explicit form of 11 by decomposing dynamical terms from $\ddot{\boldsymbol{x}}$, $\dot{\boldsymbol{x}}$.

$$\boldsymbol{M}(x)\ddot{\boldsymbol{x}} + \boldsymbol{H}(\boldsymbol{x}, \dot{\boldsymbol{x}}) + \boldsymbol{G}(x) = \boldsymbol{J}^T\boldsymbol{\tau} \tag{11}$$

in which, $\boldsymbol{M}$ is the mass matrix, $\boldsymbol{H}$ is the vector of Coriolis and centrifugal terms, and $\boldsymbol{G}$ is the vector of gravity forces. These explicit dynamical equations can be solved with usual numerical integration routines such as Runge-Kutta methods [25].

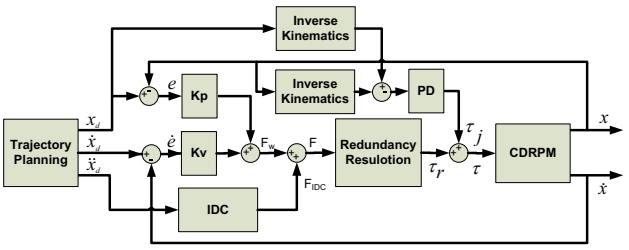

Fig. 3. The integrated control scheme

III. Control

Due to closed-chain kinematics, redundancy, and nonlinear dynamics, the CDRPMs have complex nonlinear behavior. A variety of controllers are proposed for these types of manipulators in the literature. However, there exist two main control topologies which are popular and most applicable due to their simplicity [5] and [26].

First, a joint space PD controller, proposed by Kawamura et al [18], is applied for the SEGESTA robot [5] and the KNTU CDRPM [26]. The resultant tracking error was $1.5 \times 10^{-3}m$ and $0.35 \times 10^{-3}(deg)$ for translation and rotation respectively. A joint space controller can not achieve the desired high performance, because the end-effector position is not measured and the coupled behavior of the cables and its total effect on the position of the end-effector is ignored. Additionally, the linear dynamic forces of the end-effector in the task coordinate are projected onto the joint coordinate. This fact degrades the performance of linear controller.

Next, a workspace PD controller is employed for tracking a desired trajectory; the resulting order of errors is the same

as joint space controller [26]. The controller based on the workspace coordinates should compensate the nonlinear dynamic behavior of the cables arising from projecting the parameters in cable coordinates onto work space coordinates, so it's apparent that a joint space controller can achieve a better performance in this area. Therefore, in order to achieve a high tracking performance, the advantages of both workspace and joint space controllers must be incorporated. Based on this idea, an integrated control scheme is proposed in this section. In the following subsections first the topology proposed for the integrated controller is elaborated, and then, controller stability is analyzed. Finally, simulation results and their analysis are presented in detail.

A. The Integrated Control

The block diagram of the integrated control is shown in figure 3. In this control scheme, two control loops are used, namely, the internal loop, which is based on decentralized PD controller in joint space and the external loop, which is based on a decentralized PD controller in workspace. Inherent nonlinear behavior of the cable manipulator is controlled by the internal loop, while external loop can effectively reduce the target tracking errors of the end-effector in the presence of disturbance force/torques. The gains of each controller are tuned such that the required tracking performance is achieved. Note that in this topology the redundancy resolution block is elaborated in section III-B.

Assume that the desired path of the manipulator in 3D is cylindrical as shown in figure 4. As illustrated in figure 3 the vector force, $\mathcal{F}$, in the external loop is determined by:

$$\mathcal{F} = \mathcal{F}_w + \mathcal{F}_{IDC} \tag{12}$$

Where $\mathcal{F}_w$ is the created vector force by PD controller $\mathcal{F}_w = K_{pw}e(t) + K_{vw}\dot{e}(t)$. Where $e(t) = x_d(t) - x(t)$ is the trajectory tracking error and K_{pw}, K_{vw} are appropriate position and velocity gain matrices, whose values in the simulations are $10^4 \times \boldsymbol{I}_{6\times6}$ and $10^3 \times \boldsymbol{I}_{6\times6}$m respectively. $\mathcal{F}_{IDC}$ is the generated vector force by the IDC [27]. Inverse dynamics generated force, preserves the end-effector current state of acceleration and obtains required force in the external loop in the form of a feedback linearization:

$$\mathcal{F}_{IDC} = \hat{M}\ddot{x}_d + \hat{G} \tag{13}$$

Where, $\hat{M}\ddot{x}, \hat{G}$ are the computed inertia and gravity forces of the end-effector represented in task coordinate. In the internal loop, the cables length L are measured and its time derivative $\dot{L}$ are either measured or estimated. Let $L_d, \dot{L}_d$ denote the desired cable length and its velocity which can be easily obtained through computing the inverse kinematics. In this part, the control efforts are directly applied through the cable driver units. In this loop, the control law is as follows:

$$\boldsymbol{\tau} = \boldsymbol{\tau}_j + \boldsymbol{\tau}_r \tag{14}$$

In which, $\boldsymbol{\tau}$ is an 8×1 tension force vector along each cable, $\boldsymbol{\tau}_r$ is redundancy resolution distributed forces vector and $\boldsymbol{\tau}_j$ is part of the tension force in the joint space coordinate that is provided by PD controller by $\boldsymbol{\tau}_j = K_{pj}e + K_{vj}\dot{e}$. The values of K_{pj} and K_{vj} which is used in the simulations are $2 \times 10^5 \times \boldsymbol{I}_{8\times8}$ and $2 \times 10^4 \times \boldsymbol{I}_{8\times8}$, respectively. These gains are tuned such that the required tracking performance is achieved. Let $e(t) = L_d - L$ and $\dot{e}(t) = \dot{L}_d - \dot{L}$ denote the error of actual cable length to that of the desired one and its derivative.

The tracking performance of the CDRPM using the proposed integrated controller is illustrated in figure 5. As seen in this figure, the proposed control topology is capable of reducing the tracking errors less than $4\mu m$ in position and less than 4×10^{-5} degrees in orientation. In order to compare the tracking performance of this control topology to that of a single loop controller, consider the two and infinity norms of the tracking performance as shown in figure 7, and notice the logarithmic scale that is used to represent the errors. As it is seen from this chart this proposed topology can significantly improve the tracking error norms in all the translational and rotational degrees of freedom. This significant improvement is due to the fact that the internal loop has a linearizing effect on the system, while the external loop ensures better tracking of the robot manipulator.

B. Redundancy Resolution

Actuator redundancy of CDRPMs is an inherent requirement in order to move the end-effector by tension forces of the cables. Redundancy resolution is an essential tool to optimally project a desired wrench in the cartesian space on the cable forces into the joint space. The KNTU CDRPM uses 8 actuators in a 6 dimensional motion. Therefore, there

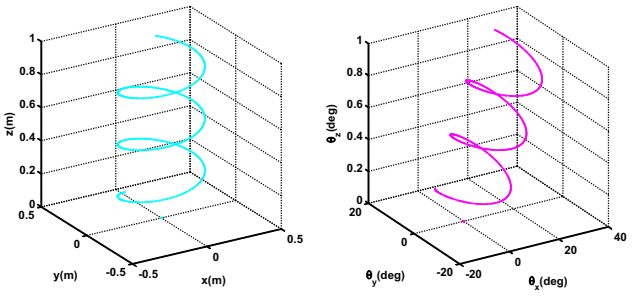

Fig. 4. Desired path in the workspace

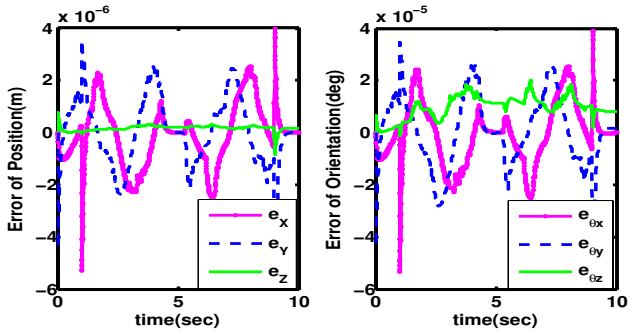

Fig. 5. The tracking error in the cascade controller

are infinitely many solutions for the eight actuators forces to solve the six dynamic equations. Let us denote the resulting cartesian force/torque applied to the manipulator moving platforms $\mathcal{F}$. In this definition $\mathcal{F}$ is calculated from the summation of all inertial, and external forces *excluding the actuator torques* $\boldsymbol{\tau}$ in the dynamic equations 10. Due to the projection property of the Jacobian matrix [21], $\mathcal{F} = \boldsymbol{J}^T\boldsymbol{\tau}$ is the projection of the actuator forces onto the moving platform, and can be uniquely determined from the dynamic equations by excluding the actuator forces from them. If the manipulator has no redundancy in actuation, the Jacobian matrix, $\boldsymbol{J}$, would be squared and the actuator forces could be uniquely determined by $\boldsymbol{\tau} = \boldsymbol{J}^{-T}\mathcal{F}$, provided that $\boldsymbol{J}$ is nonsingular. For redundant manipulators, however, there are infinity many solution for $\boldsymbol{\tau}$ to be projected into $\mathcal{F}$. The simplest solution is a minimum norm solution, which can be determined by the pseudo–inverse of $\boldsymbol{J}^T$, through:

$$\boldsymbol{J}^{T^\dagger} = \boldsymbol{J}^T(\boldsymbol{J}.\boldsymbol{J}^T)^{-1} \tag{15}$$

By this means, $\boldsymbol{\tau}_0 = \boldsymbol{J}^{T^\dagger}\mathcal{F}$ determines the minimum required force of each cable to generate the corresponding force, $\mathcal{F}$. However, this solution can result into positive or negative tensions of the cables. Since the cable forces must be kept in tension in all maneuvers, a constrained optimization technique is proposed in here to resolve the redundancy. Note that all the solutions of the projection can be determined using the null space of the Jacobian matrix by:

$$f_\tau(\boldsymbol{\gamma}) = \boldsymbol{\tau}_0 + \left(\boldsymbol{I}_{m\times m} - \boldsymbol{J}^{T^\dagger}.\,\boldsymbol{J}^T\right)\boldsymbol{\gamma} \tag{16}$$

in which, $\boldsymbol{I}$ is the identity matrix and $\boldsymbol{\gamma}$ is an m dimensional vector in the joint space. $f_\tau(\boldsymbol{\gamma})$ determines an affine hyperplane as an intersection of n subspaces of linear equality constraint defined by Jacobian transpose. To achieve a solution for the actuator forces of the CDRPM, the constrained optimization is numerically solved in order to find an optimum value for $f_\tau(\boldsymbol{\gamma})$ by finding an appropriate value for $\boldsymbol{\gamma}$ vector in the equation 16. In this optimization the norm of actuator efforts are minimized subject to:

$$\boldsymbol{\tau} = f_\tau(\boldsymbol{\gamma}) \Rightarrow (\forall i, i \in \{1, 2, \ldots, m\} \Rightarrow \boldsymbol{\tau}_i > \tau_{min}) \tag{17}$$

where, τ_{min} is the lower bound of the actuator forces. Other optimization techniques can be used to find the actuator forces projected from, $\mathcal{F}$ which can minimize another user defined cost function [8].

The simulation result for the cascade controller using the proposed redundancy resolution scheme is shown in figure 6. As it is seen the proposed redundancy resolution scheme is capable to keep the actuator forces of the CDRPM always positive.

C. Stability Analysis

In this subsection, the stability of CDRPMs under the integrated control law is proved by Lyapunov stability theorem. First, the dynamic equation of error is derived. Regarding dynamic equation of the manipulator from 11 and the control law from 14, we have:

$$\begin{aligned}\boldsymbol{M}\ddot{x} + \boldsymbol{H} + \boldsymbol{G} &= K_{pw}(x_d - x) + \boldsymbol{M}\ddot{x_d} + \boldsymbol{G} \\ &\quad + \boldsymbol{J}^T\Big(K_{pj}(l_d - l) + K_{vj}(\dot{l_d} - \dot{l})\Big)\end{aligned} \tag{18}$$

or,

$$\boldsymbol{M}\ddot{e} + K_{pw}e + K_{vw}\dot{e} + \boldsymbol{J}^T K_{pj}e_l + \boldsymbol{J}^T K_{vj}\boldsymbol{J}\dot{e} + \boldsymbol{H} = 0 \tag{19}$$

which results in:

$$\boldsymbol{M}\ddot{e} + (K_{vw} + \boldsymbol{J}^T K_{vj}\boldsymbol{J})\dot{e} + K_{pw}e + \boldsymbol{J}^T K_{pj}e_l + \boldsymbol{H} = 0 \tag{20}$$

in which, $e = x_d - x$ and $e_l = l_d - l$ and $(.)_d$ is a notation for desired values. Now, consider the following Lyapunov function:

$$\boldsymbol{V} = \frac{1}{2}\dot{e}^T\boldsymbol{M}\dot{e} + \frac{1}{2}e_l^T K_{pj}e_l + \frac{1}{2}e^T K_{pw}e \tag{21}$$

Where $\boldsymbol{M}$, $\boldsymbol{K}_pw$ and $\boldsymbol{K}_pj$ are positive definite matrices.The time derivation of Lyapunov function $\boldsymbol{V}$ is given by

$$\dot{\boldsymbol{V}} = \dot{e}^T\boldsymbol{M}\ddot{e} + \frac{1}{2}\dot{e}^T\dot{\boldsymbol{M}}\dot{e} + \dot{e_l}^T K_{pj}e_l + \dot{e}^T K_{pw}e \tag{22}$$

By substituting $\boldsymbol{M}\ddot{e}$ from the dynamic equation of error in equation 20, we have:

$$\begin{aligned}\dot{\boldsymbol{V}} = \dot{e}^T\Big(&-(K_{vw} + \boldsymbol{J}^T K_{vj}\boldsymbol{J})\dot{e} - K_{pw}e + \boldsymbol{J}^T K_{pj}e_l - \boldsymbol{H}\Big) \\ &+ \frac{1}{2}\dot{e}^T\dot{\boldsymbol{M}}\dot{e} + \dot{e_l}^T K_{pj}e_l + \dot{e}^T K_{pw}e\end{aligned} \tag{23}$$

$$\dot{\boldsymbol{V}} = -\dot{e}^T(K_{vw} + \boldsymbol{J}^T K_{vj}\boldsymbol{J})\dot{e} + \frac{1}{2}\dot{e}^T(\dot{\boldsymbol{M}} - 2\boldsymbol{H})\dot{e} \tag{24}$$

$$\dot{\boldsymbol{V}} = -\dot{e}^T(K_{vw} + \boldsymbol{J}^T K_{vj}\boldsymbol{J})\dot{e} \tag{25}$$

where, $\boldsymbol{J}^T K_{vj}\boldsymbol{J}$ is a positive definite matrix, because K_{vj} is positive definite and:

$$y^T\left(\boldsymbol{J}^T K_{vj}\boldsymbol{J}\right)y = y^T\left(\boldsymbol{J}^T K_{vj}^{\frac{1}{2}} K_{vj}^{\frac{1}{2}}\boldsymbol{J}\right)y = z^T z > \mathbf{0}$$

Therefore, $K_{vw} + \boldsymbol{J}^T K_{vj}\boldsymbol{J}$, the sum of two PD matrices, is a PD matrix; Then we can conclude that $\dot{\boldsymbol{V}} \leq 0$. Thus, the motion converges to a maximum invariant set which satisfies $\dot{\boldsymbol{V}} = 0$. In this case, $\dot{\boldsymbol{V}} = 0$ means that $\dot{e} = 0$. Therefore, due to the equation 20, the maximum invariant set is:

$$(K_{pw} + \boldsymbol{J}^T K_{pj}\boldsymbol{J})e = 0 \tag{26}$$

From positive definiteness of $(\boldsymbol{K}_{pw} + \boldsymbol{J}^T\boldsymbol{K}_{pj}\boldsymbol{J})$, this leads to $\boldsymbol{e} = 0$. Hence, we conclude: $\boldsymbol{x} = \boldsymbol{x}_d$ as time t tends to infinity as long as the motion is within the wrench closure workspace [7] and without any collision [28] parallel or serial type singularity.

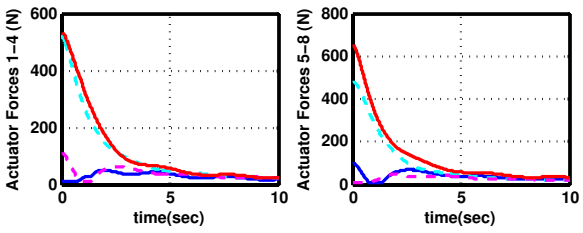

Fig. 6. The actuator forces in the cascade controller

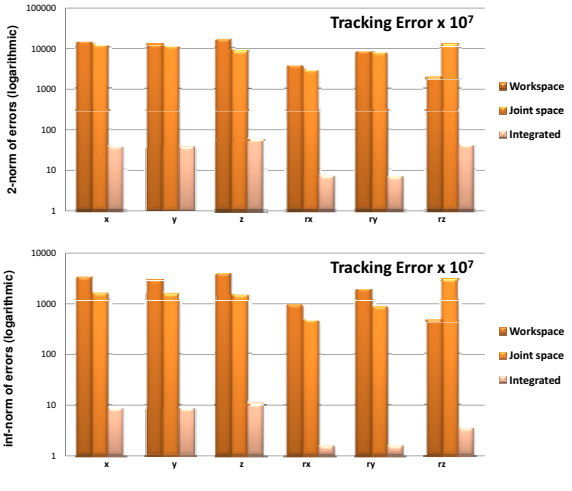

Fig. 7. Comparison of norms between three control topologies

IV. Conclusion

An integrated control strategy is proposed to improve the overall tracking performance of a cable driven redundant parallel manipulator while system nonlinear behavior is remedied and sensitivity of the external loop to nonlinearity of the cables dynamics is decreased. The main idea in this controller algorithm is the integration of two control loops, namely the internal loop, which is based on decentralized PD controller in the joint space and the external loop, which is based on a decentralized PD controller in the workspace. Inherent nonlinear behavior of the cable manipulator is significantly reduced by internal loop, while the external loop can effectively reduce the tracking errors of the end-effector in the presence of disturbance force/torques. The work presented here represents an effective attempt to use two control loops for performance improvement in trajectory-following tasks of this type of robot manipulators. The simulation analysis presented on the KNTU CDRPM verifies the expected theoretical claims and demonstrated that the proposed algorithm can significantly improve the overall tracking performance while keeping the cables under positive tension. As shown in figure 7 the cascade strategy can decrease the tracking error by 80% with respect to the previously advised inverse dynamic control. The investigated control topologies can be carefully implemented for the other cable parallel redundant manipulators in real–time applications.

References

[1] C. M. Gosselin, "Dexterity indices for planar and spatial robotic manipulators," *IEEE International Conference on Robotics and Automation*, 1990.

[2] S.-H. Lee, J.-B. Song, W.-C. Choi, and D. Hong, "Position control of a stewart platform using inverse dynamics control with approximate dynamics," *Mechatronics*, vol. 13, pp. 605–619, 2003.

[3] S. Tadokoro and T. Matsushima, "A parallel cable-driven motion base for virtual acceleration," in *Int. Conf. IROS*, pp. 1700–1705, November 2001.

[4] S. Song and D. Kwon, "Geometric formulation approach for determining the actual solution of the forward kinematices of 6-dof parallel manipulators," in *IEEE Int. Conf. IROS*, pp. 1930–1935, 2002.

[5] S. Fang, D. Franitza, M. Torlo, F. Bekes, and M. Hiller, "Motion control of a tendon-based parallel manipulators using optimal tension distribution," *IEEE/ASME Transactions on Mecatronics*, vol. 9, pp. 561–568, September 2004.

[6] C. Pham, S. Yeo, G. Yang, M. Kurbanhusen, and I. Chen, "Force-closure workspace analysis of cable-driven parallel mechanisms," *Mechanism and Machine Theory*, vol. 41, pp. 53–69, 2006.

[7] A. Zarif, M. M. Aref, and H. D. Taghirad, "Wrench feasible workspace analysis of cable-driven parallel manipulators using LMI approach." IEEE/ASME International Conference on Advanced Intelligent Mechatronics (AIM), May 2009.

[8] T. Bruckmann, L. Mikelsons, M. Hiller, and D. Schramm, "A new force calculation algotithm for tendon-based parallel manipulators," in *IEEE Conf. on Advanced Intelligent Mechatronics*, pp. 1–6, September 2007.

[9] H. Guo, Y. Liu, G. Liu, and H. Li, "Cascade control of a hydraulically driven 6-dof parallel robot manipulator based on a sliding mode," *Control Engineering Practice*, 2007.

[10] H. Kim, Y. Cho, and K. Lee, "Robust nonlinear task space control for 6dof parallel manipulator," *Automatica*, vol. 41, no. 9, pp. 1591–1600, 2005.

[11] Y. Su, D. Sun, L. Ren, and J. Mills, "Integration of saturated pi synchronous control and pd feedback for control of parallel manipulators," *IEEE Transactions on Robotics*, vol. 22, pp. 202–207, February 2006.

[12] F. Ghorbel, O. Chetelat, R. Gunawardana, and R. Longchamp, "Modeling and set point control of closed-chain mechanisms: Theory and experiment," *IEEE Transactions on Control Syst. Technol.*, vol. 8, p. 801815, September 2000.

[13] P. Chiacchio, F. Pierrot, L. Sciavicco, and B. Siciliano, "Robust design of independent joint controllers with experimentation on a high-speed parallel robot," *IEEE Transactions on Ind. Electron.*, vol. 40, p. 393403, August 1993.

[14] B. Zi, B. Duan, J. Du, and H. Bao, "Dynamic modeling and active control of a cable-suspended parallel robot," *Mechatronics*.

[15] Z. Pei, Y. Zhang, and Z. Tang, "Model reference adaptive pid control of hydraulic parallel robot based on rbf neural network," in *IEEE International Conference on Robotics and Biomimetics*, pp. 1383–1387, December 2007.

[16] E. Fasse and C. Gosselin, "Spatio-geometric impedance control of goughstewart platforms," *IEEE Transactions on Robot. Autom.*, vol. 15, p. 281288, April 1999.

[17] V. Duchine, S. Bouchard, and C. M. Gosselin, "Computationally efficient predictive robot control," *IEEE/ASME Transactions On Mechatronics*, vol. 12, pp. 570–578, October 2007.

[18] S. Kawamura, H. Kino, and C. Won, "High-speed manipulation by using parallel wire-driven robots," *Robotica*, pp. 13–21, 2000.

[19] H. Kino, T. Yahiro, F. Takemura, and T. Morizono, "Robust pd control using adaptive compensation for completely restrained parallel-wire driven robots: translational systems using the minimum number of wires under zero-gravity condition," *IEEE Transactions on Robotics*, vol. 23, pp. 803–812, Agust 2007.

[20] L. Yingjie, Z. Wenbai, and R. Gexue, "Feedback control of a cable-driven goughstewart platform," *IEEE Transactions on Robotics*, vol. 22, pp. 198–202, February 2006.

[21] L. Tsai, *Robot Analysis*. John Wiley and Sons ,Inc, 1999.

[22] J. Merlet, *Parallel Robots*. Springer, 2006.

[23] M. M. Aref, P. Gholami, and H. D. Taghirad, "Dynamic analysis of the KNTU CDRPM: a cable driven redundant manipulator," in *IEEE/ASME International Conference on Mechtronic and Embedded Systems and Applications (MESA)*, pp. 528–533, 2008.

[24] X. Diao and O. Ma, "Workspace analysis of a 6-dof cable robot for hardware-in-the-loop dynamic simulation," in *IEEE/RSJ Int.Conf. IROS*, pp. 4103–4108, 2006.

[25] L. F. Shampine, *Numerical solution of ordinary differential equations*. Chapman & Hall, 1994.

[26] P. Gholami, M. M. Aref, and H. D. Taghirad, "On the control of the KNTU CDRPM: A cable driven parallel manipulator," in *IEEE/RSJ Int. Conf. IROS*, pp. 2404–2409, September 2008.

[27] H. Asada and J. Slotine, *Robot Analysis and Control*. John Wiley and Sons, 1985.

[28] M. Aref and H. Taghirad, "Geometrical workspace analysis of a cable-driven redundant parallel manipulator: KNTU CDRPM," in *IEEE Int.Conf. IROS*, pp. 1958–1963, September 2008.